

Entanglement dynamics of spin systems in pure states

G. B. Furman, V. M. Meerovich, and V. L. Sokolovsky

Department of Physics, Ben Gurion University, Beer Sheva 84105, Israel

(Received 23 June 2009; published 16 September 2009)

We investigate numerically the appearance and evolution of entanglement in spin systems prepared initially in a pure state. We consider the dipolar coupling spin systems of different molecular structures: benzene C_6H_6 , cyclopentane C_5H_{10} , sodium butyrate $CH_3(CH_2)_2CO_2Na$, and calcium hydroxyapatite $Ca_5(OH)(PO_4)_3$. Numerical simulations show that the close relationship exists between the intensity of second order (2Q) coherences and concurrences of nearest spins in a cyclopentane molecule.

DOI: [10.1103/PhysRevA.80.032316](https://doi.org/10.1103/PhysRevA.80.032316)

PACS number(s): 03.67.Mn, 76.60.-k

I. INTRODUCTION

Quantum entanglement, the most characteristic feature of quantum mechanics, is one of the central concepts in quantum information theory and is the feature that distinguishes it most significantly from the classical theory. Entanglement is now viewed as a physical resource, which provides a means to perform quantum computation and quantum communication [1–4]. Entanglement, as the quantum correlation, can bring up richer possibilities in the various fields of modern technology. Therefore, great efforts have been made in the past few years to understand and create entanglement. Entanglement between two systems can be generated if they interact in a controlled way [5]. However, in most real experiments, specific conditions for creation of the entangled states are requested. It has recently been shown that, in two- and three-spin [6] and in many-spin [7,8] clusters of protons, the entangled state of a spin pair is emerged only at very low temperatures $T \approx 20$ mK. The same extreme conditions are required to achieve a pure state, where the populations of all quantum states except only one quantum state are equaled to zero [9,10]. The pure state is usually used as a starting point for the quantum computation, communication, and teleportation algorithms. To overcome the experimental problems related to very high magnetic fields and extremely low temperatures, a so-called pseudopure state was introduced [9–11]. In this state populations of all the quantum states except one of them are the same but nonzero which can be represented in the following form [10]:

$$\rho_{ps} = \frac{1 - \alpha}{2^N} \hat{I} + \alpha \rho_p \quad (1)$$

for ρ_p a pure. Here \hat{I} is the identity operator and α is parameter which depends on experimental conditions and number of spins N . Equation (1) describes the pure state at $\alpha=1$.

Many methods have been proposed to prepare the pseudopure state such as temporal averaging [12], spatial averaging [13], logical labeling [14], and cat-benchmark [15]. All these methods used transition-selective or qubit-selective pulses. Therefore, the size of a spin ensemble that can be prepared in the pseudopure state has been limited by spectral resolution and the signal-to-noise (S/N) ratio.

Recently, an elegant method of creating pseudopure states starting from the thermal equilibrium state was proposed, which does not require a resolved equilibrium spectrum [16].

The method is based on multiple-quantum (MQ) dynamics with filtering of the highest order multiple-quantum coherence. The method has been successfully used to prepare a pseudopure state in clusters of benzene molecules in liquid-crystalline solvent: (1) six homonuclear spins, (2) seven-heteronuclear dipolar-coupled spins with single labeled ^{13}C , and (3) twelve-heteronuclear dipolar-coupled spins with full labeled ^{13}C [17,18].

Following this method, we have formulated in [19] the strategy of preparation of a pseudopure state: (1) excitation of MQ coherences starting from the thermal equilibrium state and lasting until the time when the intensity of zeroth-order coherence is reduced to zero; (2) filtering of the highest order multiple-quantum coherence. This strategy was proved by the numerical simulation with real molecular structures, such as a rectangular (1-chloro-4-nitrobenzene molecule), a chain (hydroxyapatite molecule), a ring (benzene molecule), and a double ring (cyclopentane molecule) [19]. This opens the way to the experimental testing. The behavior of a density matrix of spin system in the pseudopure state is exactly the same as the behavior of the pure one [10,11] because they differ only on the scaled unit matrix which does not contribute to observables and it is not changed by unitary evolution transformations. At the same time, entanglement depends on whether the state of the spin system is pure [$\alpha=1$ in Eq. (1)] or pseudopure [20,21]. It is possible to obtain bounds on the value of α for which the state in Eq. (1) is entangled [20,21]. For example, asymptotic upper bound on the size of the neighborhood of separable density matrices that is of order $\alpha \approx 2^{-N/2}$ [20]. In typical NMR experiments $\alpha \approx 10^{-2}$ for ten spins, a value which is too small for this state to be entangled [20,21].

Recently, it has been suggested [22,23] to perform the MQ NMR experiments on spin systems being in the pseudopure state. As a result of using the pseudopure initial condition, many-spin correlations in clusters appear faster [22,23] than in the ordinary MQ NMR experiments [24].

In the present paper we consider an application of the MQ NMR technique for creation of entanglement in systems initially prepared in the pure state. Results of computer simulations of entanglement dynamics are presented for real structures which were used in NMR and MQ NMR experiments (six protons of benzene molecule C_6H_6 [16], ten protons of cyclopentane molecule C_5H_{10} [25], a chain of four carbons of fully ^{13}C -labeled sodium butyrate

$\text{CH}_3(\text{CH}_2)_2\text{CO}_2\text{Na}$ [26] and protons of calcium hydroxyapatite $\text{Ca}_5(\text{OH})(\text{PO}_4)_3$ [27]). Below we describe the MQ NMR technique applied to the spin system initially is in the pseudopure or pure state.

II. MQ NMR IN THE PSEUDOPURE AND PURE STATES

The interaction energy of a system of nuclear dipolar-coupled spins in a typical NMR field of 2–10 T can be represented by the secular part of the dipolar Hamiltonian ($\hbar=1$),

$$H_D = \sqrt{6} \sum_{j < k} D_{jk} T_{20}^{jk}, \quad (2)$$

where $D_{jk} = \gamma^2 \hbar / r_{jk}^3 (1 - 3 \cos^2 \theta_{jk})$ is the coupling constant between spins j and k , γ is the gyromagnetic ratio, r_{jk} is the distance between spins j and k , θ_{jk} is the angle between the internuclear vector \vec{r}_{jk} and the external magnetic field, T_{20}^{jk} is the zero component of a normalized irreducible spherical tensor of rank 2, which, in terms of the projection of the individual spin angular momentum operators $I_{j\alpha}$ on the axis α ($\alpha=x, y, z$), is [28]

$$T_{20}^{jk} = \frac{1}{\sqrt{6}} \left[2I_{jz}I_{kz} - \frac{1}{2}(I_j^+ I_k^- + I_j^- I_k^+) \right], \quad (3)$$

where I_j^+ and I_j^- are the raising and lowering operators of spin j .

The basic scheme of MQ NMR experiment consists of four distinct periods of time: preparation (τ), evolution (t_1), mixing (τ), and detection [24]. The efficient multiple quantum pulse sequence contains eight-pulse cycle [24]. The preparation period is necessary to create MQ coherences. In the rotating reference frame [29], the average Hamiltonian H_{MQ} describing the MQ dynamics at the preparation period can be written as [24,30]

$$H_{MQ} = H^{(2)} + H^{(-2)},$$

$$\text{where } H^{(\pm 2)} = -\frac{1}{4} \sum_{j < k} D_{jk} I_j^\pm I_k^\pm. \quad (4)$$

The density matrix of the spin system, $\rho(\tau)$, at the end of the preparation period is

$$\rho(\tau) = U(\tau)\rho(0)U^\dagger(\tau), \quad (5)$$

where $U(\tau) = \exp(-i\tau H_{MQ})$ is the evolution operator acting during the preparation period and $\rho(0)$ is the initial density matrix of the system.

Usually the thermodynamical equilibrium density matrix is used as the initial one for MQ NMR experiments [24] and the equilibrium spin density matrix ρ_{eq} has the following form: $\rho_{eq} = \exp(-\omega I_z / kT)$ [28,29] where ω is the Zeeman splitting and kT is the thermal energy and $I_z = \sum_{j=1} I_{jz}$. In the high temperature limit ($\omega \ll kT$) this simplifies to $\rho_{eq} = I_z$ [29].

Here we consider MQ NMR dynamics with the initial pseudopure state (1) and the pure state when the density matrix can be described as

$$\rho_p(0) = |1\rangle_1 \otimes |1\rangle_2 \otimes \dots \otimes |1\rangle_N, \quad (6)$$

where $|1\rangle_k$ represents the k th spin that is up and N is the number of spins in the system.

The resulting signal after the mixing period, the longitudinal magnetization, $M_z(t)$, is

$$M_z(t) = \text{Tr}\{\rho(t)I_z\}, \quad (7)$$

where

$$\rho(t) = U^\dagger(\tau) e^{-i\Delta\omega t I_z} \rho(\tau) e^{i\Delta\omega t I_z} U(\tau), \quad (8)$$

where $\rho(\tau)$ is the density matrix at the end of the preparation period according to Eq. (5) and $t=2\tau+t_1$, $\Delta\omega$ is the frequency offset on the evolution period of the duration t_1 which is a result of applying the time proportional phase incrementation method [24]. One can rewrite the expression for the observable signal in terms of the intensities of MQ coherences,

$$M_z(t) = \sum_n e^{-in\Delta\omega t} J_n(\tau), \quad (9)$$

where $J_n(\tau)$ are the normalized intensities of MQ coherences in the pseudopure state or in the pure state [23]. At this consideration, we can neglect the scaled unit matrix because it does not contribute to observables and it is not changed by unitary evolution transformations.

The sum of the intensities of all MQ coherences is time independent: $\sum_n J_n(\tau) = 1$ and $J_n(\tau) = J_{-n}(\tau)$ [23]. Note that it is not necessary to make any changes in the scheme of the standard experiment in order to obtain nonzero signals of MQ coherences in the pseudopure state or in the pure state [23].

III. ENTANGLEMENT MEASURE AND REDUCED DENSITY MATRIX

To study the entanglement dynamics, we will use a measure of entanglement of two spins in the form of the entropy of formation [31]:

$$E_F[\rho_{mn}(\tau)] = \text{Tr}[\rho_{mn}(\tau) \ln \rho_{mn}(\tau)], \quad (10)$$

where $\rho_{mn}(\tau)$ is the reduced density matrix describing dynamics of the m th and n th spins. This matrix is defined by

$$\rho_{mn}(\tau) = \text{Tr}_{mn}[\rho(\tau)], \quad (11)$$

where $\text{Tr}_{mn}(\dots)$ denotes the partial trace over the degrees of freedom for all the spins except the m th and n th ones, $\rho(\tau)$ is the density matrix just after the preparation period [Eq. (5)]. The relation between E_F and the concurrence between two spins C is given by

$$E_F(x) = -x \log_2 x - (1-x) \log_2 (1-x), \quad (12)$$

where $x = \frac{1}{2}(1 + \sqrt{1 - C^2})$ [31]. For the maximally entangled states, the concurrence is $C=1$ while for separable states $C=0$.

The concurrence between spins m and n is expressed by the formula

$$C_{mn} = \max \left\{ 0, 2\lambda_{mn} - \sum_{k=1}^4 \lambda_{mn}^{(k)} \right\}, \quad (13)$$

where $\lambda_{mn} = \max\{\lambda_{mn}^{(k)}\}$ and $\lambda_{mn}^{(k)} (k=1, 2, 3, 4)$ are the square roots of the eigenvalues of the product

$$R_{mn}(\tau) = \rho_{mn}(\tau)(\sigma_y \otimes \sigma_y) \tilde{\rho}_{mn}(\tau)(\sigma_y \otimes \sigma_y). \quad (14)$$

Here $\tilde{\rho}_{mn}(\tau)$ is the complex conjugation of $\rho_{mn}(\tau)$ and $\sigma_y = \begin{pmatrix} 0 & -i \\ i & 0 \end{pmatrix}$ is the Pauli matrix.

IV. NUMERICAL SIMULATION OF ENTANGLEMENT DYNAMICS IN THE PURE STATE

To perform numerical simulation of entanglement dynamics of nuclear spin clusters, we will consider several systems suitable for studying by MQ NMR technique: six dipolar-coupled proton spins of benzene molecule C_6H_6 (ring of six spins) [16], ten protons of molecule cyclopentane C_5H_{10} (two pentagon cycles of ten spins) [26], a chain of four carbons of fully ^{13}C -labeled sodium butyrate $CH_3(CH_2)_2CO_2Na$ [26], and protons of calcium hydroxyapatite $Ca_5(OH)(PO_4)_3$ [30]. In our numerical simulations, the dipole-dipole interaction (DDI) constant of the nearest neighbors is chosen to be $D_{s,s+1} = D = 1 \text{ s}^{-1}$. The spin systems in molecules, such as benzene, sodium butyrate, and hydroxyapatite dissolving in liquid-crystalline matrix [16–18], can be arranged as regular circles and chains with the ratio of the DDI constants of spins s and n is given by $D[\frac{\sin(\pi/N)}{\sin[\pi(s-n)/N]}]^3$ for the ring and $D/|s-n|^3$ for the chain, respectively.

The normalized DDI constants for cyclopentane molecules (two pentagon cycles) are determined as $\bar{D}_{sn} = D_{sn}/D_{11'}$, and equal: $\bar{D}_{11'} = 1$, $\bar{D}_{12} = -0.178$, $\bar{D}_{12'} = -0.002$, $\bar{D}_{13} = -0.093$, and $\bar{D}_{13'} = -0.026$ [25]. Here the primes concern to the bottom pentagon cycle. The external dc field is directed parallel to the plane of pentagons.

The dependences of the intensities of MQ coherences on the dimensionless time $D\tau$ in cyclopentane molecule containing ten spins and initially preparing in the pseudopure state (1) are presented in Fig. 1. In the pseudopure states, the MQ coherences of the various orders can be produced (Fig. 1). At the same time the spin states are not entangled and thus the spin-spin correlations have a purely classical interpretation.

The results of the numerical simulation in the pure state are presented in Figs. 2–4. Nonzero concurrence appears in all considered spin systems. The time dependence of concurrences has quasiperiodical character. The figures present only one cycle.

One of features of the ring structure is that the most remote spins achieve large values of concurrence: $C_{14} \sim C_{12} \gg C_{13}$ (Fig. 2). Figure 3 compares the concurrences of different spin pairs for three-dimensional structure of cyclopentane: the concurrence between closest spins located at parallel planes ($C_{nn'}$) is by order of magnitude greater than the concurrence between spins located at the same plane (C_{nm} or $C_{n'm'}$). This concurrence is by two orders greater than values C_{nm} . Entanglement between remote spins appears a little

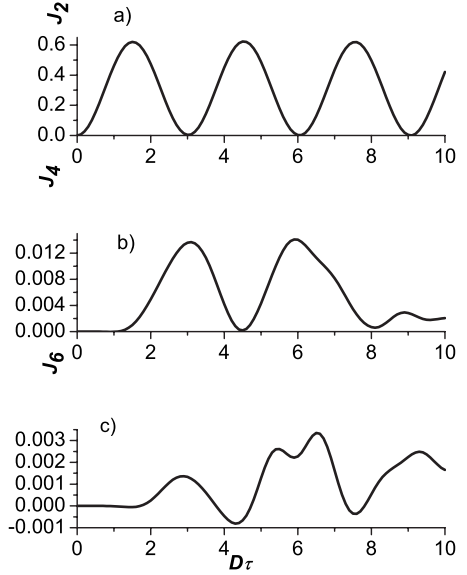


FIG. 1. Time dependence of the MQ coherences in the two pentagon rings of ten-spin system starting with the pseudopure state (1): (a) J_2 , (b) J_4 , and (c) J_6 .

later than entanglement between the closest ones. One can compare the 2Q intensity in the spin system is in pseudopure state [Fig. 1(a)] with the system is in the pure state [Fig. 3(a); red dashed line]. It is evident that initial pseudopure and pure states give exactly the identical time dependence of the intensity J_2 . The same results we obtained for the intensities J_4 and J_6 .

From point of view of the future applications to quantum communication, the most interesting case for a chain is the generation of entanglement between the spins at the ends of the chain. It is well known that, in most systems with short-

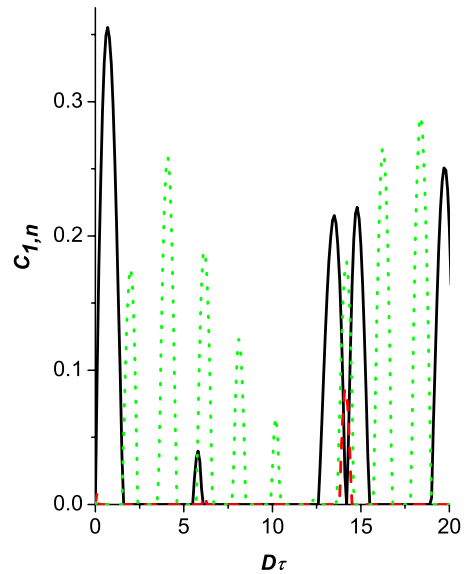


FIG. 2. (Color online) Time dependence of the concurrences C_{mn} in a six-spin ring with the pure initial state (6). Black solid line: $m=1, n=2$; red dashed line: $m=1, n=3$; green dotted line: $m=1, n=4$.

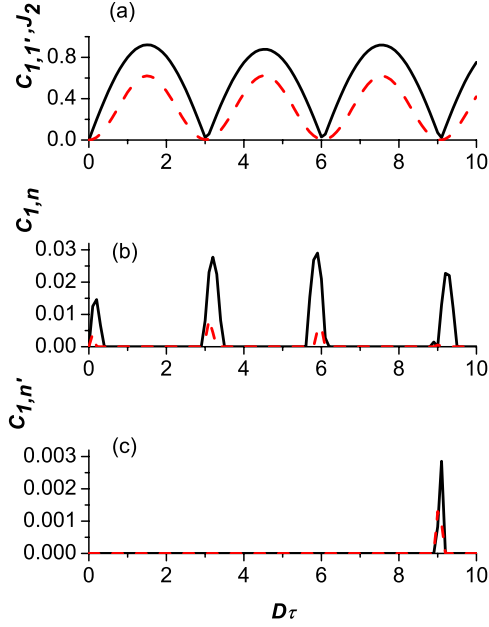


FIG. 3. (Color online) Dynamics of the concurrences C_{mn} and the intensities of the MQ coherences vs time in the two pentagon rings of ten-spin system starting with the pure initial state (6). (a) Black solid line— $n=1$ and $m=1'$; red dashed line— J_2 . (b) Black solid line— $n=1$ and $m=2$; red dashed line— $n=1$ and $m=3$. (c) Black solid line— $n=1$ and $m=2'$; red dashed line— $n=1$ and $m=3'$.

range interactions, pairwise entanglement decays rapidly with distance [32,33]. Let us consider four-, six-, and ten-spin chains where the interaction exists only between nearest neighbors. Within this approximation, the interaction Hamiltonian is truncated to the following terms:

$$H_D = J \sum_j I_{jz} I_{(j+1)z}. \quad (15)$$

Figure 3 gives time dependences of the concurrences in linear chains of four, six, and ten nuclear spins. The concurrences between the nearest-neighbor spins appear immediately: $C_{1,2}$ in Figs. 3(a)–3(c) and $C_{2,3}$ in Fig. 3(a). Then, at $\tau=1/D$, the next-neighbor spin concurrence appears, $C_{1,3}$ in Figs. 3(a)–3(c). Later, the surprising phenomenon consisting in occurrence of entanglement of the most remote spins is observed: $C_{1,4}$ in four-spin chain, $C_{1,6}$ in six-spin chain, and $C_{1,10}$ in ten-spin chain [Figs. 4(a)–4(c)]. Only after appearance of the concurrences between the spins at the ends of the chains, the concurrences between the next-next-neighbor and more distant spins are generated. In spin chains the time of achieving the first maximum of concurrences between the first and second spins as well as between the first and third spins are independent of the length of a chain (Fig. 3). In short spin chains ($N \leq 10$) the concurrences between the most remote spins reach the maximum when $D\tau = \frac{N+2}{2}$ approximately.

V. DISCUSSION AND CONCLUSIONS

A problem of identification of entanglement of a quantum state is the most fundamental problem in the field of

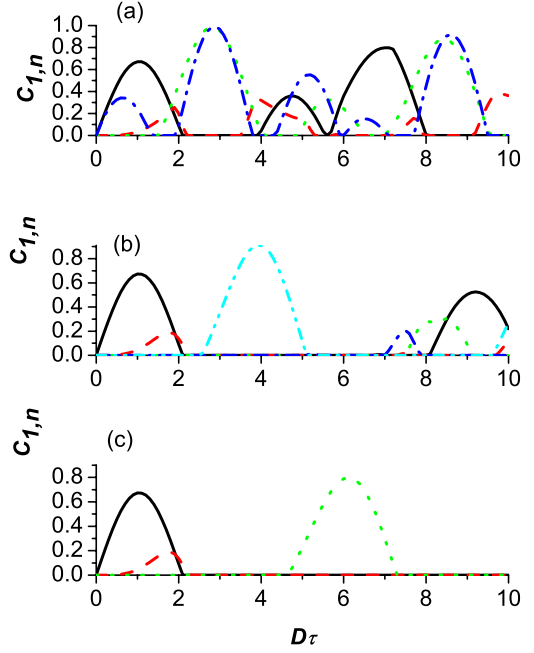


FIG. 4. (Color online) Evolution of the concurrences C_{mn} in the spin chains with DDI of the nearest neighbors and pure initial state (6). (a) Four spins: black solid line— $m=1$, $n=2$; red dashed line $m=1$, $n=3$; green dotted line $m=1$, $n=4$; blue dot-dashed line— $m=2$, $n=3$. (b) Six spins: black solid line— $m=1$, $n=2$; red dashed line $m=1$, $n=3$; green dotted line $m=1$, $n=4$; blue dot-dashed line— $m=1$, $n=5$, cyan dot-dot-dashed line $m=1$, $n=6$. (c) Ten spins: black solid line— $m=1$, $n=2$; red dashed line $m=1$, $n=3$; green dotted line $m=1$, $n=10$. Note that the concurrences C_{mn} with $m=1$ and $n=4, 5, 6, 7, 8, 9$ up to the time $\tau=10/D$ equal zero.

quantum information processing [34]. One way to decide that a state is entangled or separable is to use an entanglement witness (EW) [34,35]. An internal energy [36], magnetic susceptibility [37], magnetization [38,39], and other measurable parameters were used as EW. In particular, for the simplest system, a pair of spins $s=1/2$ coupled by DDI, it was proposed to use the intensity of MQ coherences as an EW [6].

Figure 2 illustrates the connection between the two phenomena: entanglement and 2Q coherence for cyclopentane molecules. The concurrence $C_{1,1'}$ between the nearest neighbors can be approximated by the formula $C_{1,1'} = 1.14\sqrt{J_2}$, where J_2 is the intensity of MQ coherence of the second order [Fig. 2(a)]. Since 2Q coherences can be easily measured by the nuclear magnetic resonance (NMR) technique, experimentalists are presented with an opportunity to study the dynamic properties of entanglement, i.e., the creation and evolution of entangled states. These relations can be used to distinguish the entangled state of a spin pair from separable one.

In conclusion, performing numerical simulation MQ NMR experiments with several real molecular structures, we have shown that the entanglement can be achieved if to start from the previously prepared pure state. In this study we found some interesting features of the entanglement dynamics. An unexpected behavior the concurrences between spins

at the ends of the chains was obtained in the model with direct interactions between nearest neighbors: the concurrences between the next-next-neighbor and more distant spins appear later than the concurrence between the most remote spins, $C_{1,N}$. The numerical experiments with cyclo-

pentane molecules revealed the close connection between the intensity of MQ coherences of the second order and concurrence between the between closest spins. As a result, the 2Q intensity can be used as entanglement witnesses for such systems.

-
- [1] M. A. Nielsen and I. L. Chuang, *Quantum Computation and Quantum Information* (Cambridge University Press, Cambridge, England, 2000).
 - [2] G. Benenti, G. Casati, and G. Strini, *Principles of Quantum Computation and Information* (World Scientific, Singapore, 2007), Vol. I and II.
 - [3] L. Amico, R. Fazio, A. Osterloh, and V. Vedral, *Rev. Mod. Phys.* **80**, 517 (2008).
 - [4] R. Horodecki, P. Horodecki, M. Horodecki, and K. Horodecki, *Rev. Mod. Phys.* **81**, 865 (2009).
 - [5] W. Dür, G. Vidal, J. I. Cirac, N. Linden, and S. Popescu, *Phys. Rev. Lett.* **87**, 137901 (2001).
 - [6] E. B. Fel'dman and A. N. Pyrkov, *JETP Lett.* **88**, 398 (2008).
 - [7] G. B. Furman, V. M. Meerovich, and V. L. Sokolovsky, *Phys. Rev. A* **78**, 042301 (2008).
 - [8] S. I. Doronin, A. N. Pyrkov, and É. B. Fel'dman, *JETP Lett.* **85**, 519 (2007).
 - [9] C. Ramanathan, N. Boulant, Z. Chen, D. G. Cory, I. Chuang, and M. Steffen, *Quantum Inf. Process.* **3**, 15 (2004).
 - [10] D. G. Cory, A. F. Fahmy, and A. N. D. T. F. Havel, *Proc. Natl. Acad. Sci. U.S.A.* **94**, 1634 (1997).
 - [11] N. A. Gershenfeld and I. L. Chuang, *Science* **275**, 350 (1997).
 - [12] E. Knill, I. Chuang, and R. Laflamme, *Phys. Rev. A* **57**, 3348 (1998).
 - [13] D. G. Cory, M. D. Price, and T. F. Havel, *Physica D* **120**, 82 (1998).
 - [14] L. M. K. Vandersypen, C. S. Yannoni, M. H. Sherwood, and I. L. Chuang, *Phys. Rev. Lett.* **83**, 3085 (1999).
 - [15] E. Knill, R. Laflamme, R. Martinez, and C.-H. Tsien, *Nature (London)* **404**, 368 (2000).
 - [16] J.-S. Lee and A. K. Khitrin, *Phys. Rev. A* **70**, 022330 (2004).
 - [17] J.-S. Lee and A. K. Khitrin, *Phys. Rev. Lett.* **94**, 150504 (2005).
 - [18] J.-S. Lee and A. K. Khitrin, *J. Chem. Phys.* **122**, 041101 (2005).
 - [19] G. B. Furman, *J. Phys. A* **39**, 15197 (2006).
 - [20] S. L. Braunstein, C. M. Caves, R. Jozsa, N. Linden, S. Popescu, and R. Schack, *Phys. Rev. Lett.* **83**, 1054 (1999).
 - [21] G. J. Milburn, R. Laflamme, B. C. Sanders, and E. Knill, *Phys. Rev. A* **65**, 032316 (2002).
 - [22] G. B. Furman and S. D. Goren, *J. Phys.: Condens. Matter* **17**, 4501 (2005).
 - [23] G. B. Furman, *J. Phys.: Condens. Matter* **21**, 026008 (2009).
 - [24] J. Baum, M. Munovitz, A. N. Garroway, and A. Pines, *J. Chem. Phys.* **83**, 2015 (1985).
 - [25] R. Poupko, Z. Luz, and H. Zimmermann, *J. Am. Chem. Soc.* **104**, 5307 (1982).
 - [26] J.-S. Lee, T. Adams, and A. K. Khitrin, *New J. Phys.* **9**, 83 (2007).
 - [27] G. Cho and J. P. Yesinowski, *J. Phys. Chem.* **100**, 15716 (1996).
 - [28] A. Abragam, *The Principles of Nuclear Magnetism* (Oxford University Press, London, 1961).
 - [29] M. Goldman, *Spin Temperature and Nuclear Magnetic Resonance in Solids* (Clarendon Press, Oxford, 1970).
 - [30] S. I. Doronin, I. I. Maximov, and E. B. Fel'dman, *Sov. Phys. JETP* **91**, 597 (2000).
 - [31] W. K. Wootters, *Phys. Rev. Lett.* **80**, 2245 (1998).
 - [32] S. Bose, *Contemp. Phys.* **48**, 13 (2007).
 - [33] N. Gisin, G. Ribordy, W. Tittel, and H. Zbinden, *Rev. Mod. Phys.* **74**, 145 (2002).
 - [34] M. Horodecki, P. Horodecki, and R. Horodecki, *Phys. Lett. A* **223**, 1 (1996).
 - [35] B. M. Terhal, *Phys. Lett. A* **271**, 319 (2000).
 - [36] X. Wang, *Phys. Rev. A* **66**, 034302 (2002).
 - [37] M. Wieśniak, V. Vedral, and C. Brukner, *New J. Phys.* **7**, 258 (2005).
 - [38] C. Brukner and V. Vedral, e-print arXiv:quant-ph/0406040.
 - [39] G. B. Furman, V. M. Meerovich, and V. L. Sokolovsky, *Quantum Inf. Process.* **8**, 283 (2009).